JACS
JOURNAL OF THE AMERICAN CHEMICAL SOCIETY
Article
pubs.acs.org/JACS

Probing Affinity and Ubiquitin Linkage Selectivity of Ubiquitin-Binding Domains Using Mass Spectrometry

Kleitos Sokratous,[†] Lucy V. Roach,[†] Debora Channing,[‡] Joanna Strachan,[‡] Jed Long,[§] Mark S. Searle,[§] Robert Layfield,[‡] and Neil J. Oldham*[,†]

[†]School of Chemistry, University of Nottingham, University Park NG7 2RD, U.K.
[‡]School of Biomedical Sciences, Queen's Medical Centre, University of Nottingham, Nottingham NG7 2UH, U.K.
[§]Centre for Biomolecular Sciences, School of Chemistry, University Park, University of Nottingham, Nottingham NG7 2RD, U.K.

Supporting Information

ABSTRACT: Non-covalent interactions between ubiquitin (Ub)-modified substrates and Ub-binding domains (UBDs) are fundamental to signal transduction by Ub receptor proteins. Poly-Ub chains, linked through isopeptide bonds between internal Lys residues and the C-terminus of Ub, can be assembled with varied topologies to mediate different cellular processes. We have developed and applied a rapid and sensitive electrospray ionization-mass spectrometry (ESI-MS) method to determine isopeptide linkage-selectivity and affinity of poly-Ub·UBD interactions. We demonstrate the technique using mono-Ub and poly-Ub complexes with a number of α-helical and zinc-finger (ZnF) UBDs from proteins with roles in neurodegenerative diseases and cancer. Affinities in the 2−200 μM range were determined to be in excellent agreement with data derived from other biophysical techniques, where available. Application of the methodology provided further insights into the poly-Ub linkage specificity of the hHR23A-UBA2 domain, confirming its role in Lys48-linked poly-Ub signaling. The ZnF UBP domain of isopeptidase-T showed no linkage specificity for poly-Ub chains, and the Rabex-5 MIU also exhibited little or no specificity. The discovery that a number of domains are able to bind cyclic Lys48 di-Ub with affinities similar to those for the acyclic form indicates that cyclic poly-Ub may be capable of playing a role in Ub-signaling. Detection of a ternary complex involving Ub interacting simultaneously with two different UBDs demonstrated the co-existence of multi-site interactions, opening the way for the study of crosstalk between individual Ub-signaling pathways.

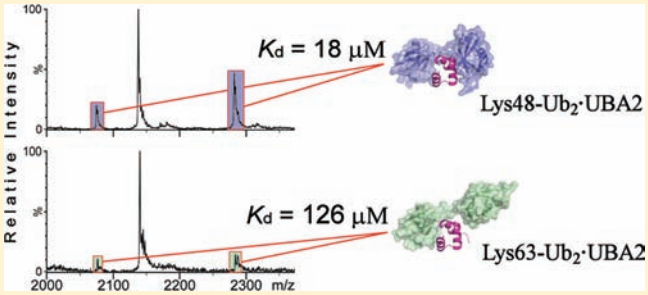

1. INTRODUCTION

Ubiquitination, a post-translational modification (PTM) resulting in the covalent attachment of ubiquitin (Ub) to a target protein, is a fundamental regulatory mechanism in many eukaryotic cellular processes. Protein degradation,[1] endocytosis,[2] vesicular trafficking,[3] cell-cycle control, DNA repair,[4] and various signaling pathways[5] are all regulated by this important PTM. Ub conjugation leads to the formation of an isopeptide bond between the C-terminal glycine carboxyl group of Ub and, usually, a lysine (Lys) residue in the target protein. Repetition of the ubiquitination cycle leads to the formation of poly-Ub chains by utilizing any one of the seven Lys residues of the Ub monomer, as well as Ub's N-terminus.[6,7] Clear evidence is emerging that proteins labeled with poly-Ub chains of a specific topology and length are driven to specific processes. For example, Lys48-linked chains classically signal for target protein degradation by the proteasome,[8] whereas Lys63-linked chains act as a trigger in a variety of pathways including DNA damage tolerance,[9] the inflammatory response,[10] protein trafficking,[11] and regulation of protein synthesis.[12]

Crucial to the function of Ub as a signaling motif is its non-covalent association with modular protein domains known as Ub-binding domains (UBDs). Examples of such include the Ub-associated (UBA) domain of human ubiquilin-1 (UQ1), a protein which acts as a presenilin regulator[13] and the UBA domains of the human homologue of yeast Rad23 (hHR23A), which mediates the delivery of substrates to the 26S proteasome,[14] including p53,[15] as well as functioning in nucleotide excision repair.[16] In contrast to the UQ1-UBA domain, which does not possess any binding preference for poly-Ub chain linkage,[17,18] the hHR23A-UBA domains are reported to show a clear selectivity for Lys48-linked over Lys63-linked poly-Ub chains.[14,18−20] Associations between the vesicular trafficking protein Rabex-5 and Ub are mediated by a zinc-finger (ZnF) module (in this case ZnF A20) and a MIU (motif interacting with Ub) domain. Whereas the MIU domain binds the Ile44-centered patch on Ub, the RUZ (Rabex-5 Ub-binding zinc finger) domain interacts with an Asp58-centered

Received: January 23, 2012
Published: March 19, 2012

 © 2012 American Chemical Society dx.doi.org/10.1021/ja300749d | J. Am. Chem. Soc. 2012, 134, 6416−6424

region.[21] A ZnF UBD (termed ZnF UBP) also contributes to interactions between free poly-Ub chains and the deubiquitinating (DUB) enzyme isopeptidase-T (IsoT or USP5), where it recognizes the C-terminal Gly residue of Ub.[22] As a result of this it is believed that the ZnF UBP domain of IsoT (hereon referred to as IsoT-ZnF) has no preference for poly-Ub chain length or topology. The specific recognition of poly-Ub chain length and topology by UBDs is only now beginning to be probed in detail. Moreover, the intrinsic importance of UBDs has also been highlighted by their recent links to a variety of pathological conditions, including cancer and immunodeficiency.[23] Further, mutations in UBDs are important in human diseases, including the skeletal disorder Paget's disease of bone.[24] Given these considerations, the development of new methods for studying Ub·UBD complexes is an area of considerable interest.

The importance of quantifying UBD binding affinities is highlighted from the observation that, for example, the Vps36 protein appears to bind Lys63-linked or linear di-Ub equally well using pull-down assays, but by fluorescence studies was found to preferably bind to the former.[25] Other methods currently employed to study Ub·UBD non-covalent complexes include nuclear magnetic resonance (NMR),[17,20,26,27] surface plasmon resonance (SPR),[19,28] isothermal titration calorimetry (ITC),[22] and fluorescence anisotropy (FA).[29] NMR and SPR experiments have been used to probe the specificity of a number of UBDs for mono-Ub and poly-Ub chains.[17,19,20,26−28] These biophysical techniques have contributed significantly to our understanding of the often weak non-covalent interactions of Ub. Both NMR and ITC require substantial quantities of protein, often at non-physiological concentrations, and are relatively low-throughput. In addition, studies on complexes where the poly-Ub·UBD non-covalent assembly exceeds 40 kDa may be very challenging by NMR. SPR is more sensitive and rapid, but can suffer from artifacts associated with immobilization of one of the protein binding partners such as avidity effects. Thus, the development of a rapid and highly sensitive method for studying the affinity and specificity of UBDs would revolutionize the study of these crucial regulatory complexes.

Electrospray ionization-mass spectrometry (ESI-MS) has emerged as a powerful analytical method for the study of protein non-covalent interactions. Several studies have successfully demonstrated its potential use as a tool to probe non-covalent complexes, where binding constants from ESI-MS experiments were shown to be in a good agreement with those obtained by other biophysical methods, such as NMR, SPR and ITC.[30−35] The measurement of solution equilibria by a gas phase method can, however, produce anomalous results; for example the determination of affinity constants for a variety of non-covalent complexes could not be obtained by ESI-MS or were found to differ from solution measurements.[36,37] These effects have often been attributed to the instability of the complex in the gas phase due to the absence of stabilizing hydrophobic effects. According to a recent paper by Liu and Konermann,[38] determination of the binding affinity for a protein−protein assembly by ESI-MS can be challenging due to potential differences in the behavior of individual and complexed proteins in the mass spectrometer. However, they show that under carefully optimized instrumental conditions, and after controlling for protein ion behavior, it is feasible to study protein−protein interactions quantitatively with this methodology.[38] The investigation of weak hydrophobic interactions seen in many Ub·UBD complexes may be expected to be difficult, but here we describe the successful development of ESI-MS as a tool, together with charge reduction methods, for the quantitative study of such interactions. We show that ESI-MS is able to report affinities in good agreement with solution data, that the complexes arise due to specific interactions between binding surfaces, and that UBD preference for poly-Ub length and topology can be revealed. In addition, we demonstrate the applicability of ESI-MS in studies of Ub ternary complexes involving multi-site UBD interactions. Together these finding demonstrate ESI-MS to be a powerful, sensitive, and broadly applicable method for studying the plethora of non-covalent interactions relevant to Ub signaling.

2. EXPERIMENTAL SECTION

2.1. Materials. Ultrapure water (18.2 MΩ·cm), obtained from a Millipore water purification system (Epsom, UK), was used in the preparation of sample solutions. Acetonitrile was purchased from ThermoFisher (Loughborough, UK). Lyophilized bovine Ub was obtained from Sigma-Aldrich (Poole, UK) and prepared as a 116 μM sample in 25 mM ammonium acetate solution (pH 6.8). Lyophilized di-Ubs (Lys11, Lys27, Lys48, and Lys63) as well as lyophilized tetra-Ubs (Lys48, Lys63) were obtained from Boston Biochem (Cambridge, MA) and prepared as 58 μM and 29 μM samples, respectively, in 25 mM ammonium acetate solution (pH 6.8). The Ub mutants, Leu8Ala/Ile44Ala and Δ-Gly75/Gly76 were prepared as described elsewhere.[39]

2.2. Expression and Purification of UBDs. All UBDs were PCR amplified from appropriate IMAGE clones (IMAGE CONSORTIUM), with the exception of IsoT-ZnF which was cloned from human U20S cDNA (a human osteosarcoma cell line). All PCR products were ligated in to the *Bam*HI/*Xho*I sites of pGEX-4T-1 (GE Healthcare). All constructs were verified by DNA sequencing. UBDs were expressed as glutathione S-transferase (GST) fusion proteins in *E. coli* strain XL10-Gold. Bacteria were grown at 37 °C in Luria broth (LB), induced with 0.2 mM isopropyl 1-thio-β-D-galactopyranoside (IPTG) at OD_{600} ~0.6, and incubated overnight at 20 °C. Cells were pelleted and lysed by sonication in 10 mM Tris, 150 mM NaCl, 0.1% (v/v) Triton X-100 (TBST), pH 7.5. The lysate was clarified by centrifugation (35000*g*, 20 min) and the supernatant was applied to a 5 mL gravity polypropylene column (Qiagen Ltd., UK) containing 130 μL of glutathione beads (glutathione Sepharose 4B, GE Healthcare, UK). After the binding of GST-UBD fusion proteins, the column was washed with thrombin cleavage buffer (TCB) (20 mM Tris, 150 mM NaCl, 2.5 mM $CaCl_2$ pH 8.4) and then incubated with 5 U of thrombin at 4 °C overnight. Released UBDs were eluted with TCB. The amino acid sequence (human) of each domain used in this study is shown in Supporting Information Table S1. The N-terminal Gly-Ser dipeptide is residual from thrombin cleavage.

2.3. Sample Preparation. UBDs were desalted and buffer exchanged into 25 mM NH_4OAc buffer using Vivaspin 500 ultrafiltration spin filters with 3 kDa (in the case of IsoT-ZnF 10 kDa) molecular weight cutoff (Sartorius, Goettingen, Germany). The IsoT-ZnF domain, subsequent to buffer exchange in 25 mM NH_4OAc, was mixed with 0.5 mM dithiothreitol (DTT) at 4 °C, 24 h prior the addition of Ub in order to reduce the disulfide-linked dimer to the monomeric domain.

Multiple replicates of six titration samples were prepared as 50:50 v/v solution mixtures to final concentrations of Ub of 0.5 μM (1 μM in the case of tetra-Ub·UQ1-UBA) and UBD (1, 2, 3, 4, 6, and 8 μM). The samples were vortexed and subjected to MS analysis with no further preparation, using a syringe pump (Harvard 22 dual syringe pump, model 55-2222 Holliston, MA, USA) and a 100 μL Hamilton syringe (Bonaduz, Switzerland), at a flow rate of 5 μL·min^{-1}.

2.4. Mass Spectrometry. Experiments were performed on a SYNAPT HDMS (Waters, Altrincham, UK), a hybrid quadrupole ion mobility time-of-flight MS instrument, with traveling-wave ion mobility (TWIM) capability, equipped with the standard z-spray

source. The instrument conditions were optimized to provide the highest relative signals for the Ub·UQ1-UBA complex sprayed from 25 mM ammonium acetate in the presence of acetonitrile vapor. The ESI capillary voltage was 2.6 kV; cone voltage, 60−80 V; extraction voltage, 5 V; transfer voltage, 5 V. The source and desolvation temperatures were adjusted to 50 °C. Cone and desolvation gas flow rates were 30 and 200 $L{\cdot}h^{-1}$, respectively. The ion mobility cell contained nitrogen gas operated at a pressure of 4.4×10^{-1} mbar. The traveling wave height and velocity were 8 V and 280 $m{\cdot}s^{-1}$, respectively. Other settings were as follow: trap and transfer collision voltage, 8 and 5 V, respectively; backing pressure, 3.8−4.2 mbar; trap pressure, 2.1×10^{-2} mbar; TOF region pressure, 1.5×10^{-6} mbar.

The ion transmission efficiency is related to the quadrupole ion transmission profile (Quad profile). The importance of using a relatively uniform transmission profile in studies of non-covalent protein-protein interactions has been recently discussed by Liu and Konermann.[38] Following a similar approach, we used these Quad profile parameters: Mass 1, 1000 m/z; Dwell 1, 5%; Ramp 1, 0%; Mass 2, 2000 m/z; Dwell 2, 55%; Ramp 2, 40%; Mass 3, 4000 m/z. Such a transmission profile should provide a relatively uniform ion transmission between m/z 1000 and 4000. Instrument control as well as data processing was performed using the Waters MassLynx 4.1 data system. All spectra were acquired in ion positive mode and the TOF analyzer operated on V-mode. Minimum smoothing and background subtraction was applied to the obtained spectra prior to analysis.

2.5. Charge Reduction by Solvent Exposure. Charge reduction was obtained by simple exposure of the electrospray plume to acetonitrile vapor.[40] A cap of a Falcon tube containing acetonitrile was placed just inside the doorway of the ESI source chamber (see Supporting Information Figure S1). Reduction of charge states on the observed spectrum occurs instantly, while recovering to usual charge states takes less than a minute by simple removal of the solvent container from the source housing.

2.6. Determination of Ub·UBD Binding Affinities by ESI-MS. Using ESI-MS, apparent K_d values for Ub·UBD complexes were determined from titration experiments. The concentration of the Ub component (mono- or poly-Ub) was fixed at 0.5 μM while the concentration of UBDs was varied from 1 to 8 μM. ESI-MS analysis of the resulting solutions was used to determine ratios (R) of signal intensities (I) attributed to free (Ub^{n+}) and UBD-bound ($Ub{\cdot}UBD^{n+}$) Ub ions. Providing that the electrospray response factors for the bound and unbound Ub ions are similar and that minimal dissociation of the complex occurs post-desolvation (see Discussion), then measured ratios represent solution equilibria. Hence the Ub·UBD binding affinity can be determined from this ratio and the initial concentration of the components, $[Ub]_0$ and $[UBD]_0$. Equations are given in the Supporting Information.

3. RESULTS

3.1. Optimization of ESI-MS Conditions. Key to the success of this method is the ability of ESI-MS to preserve Ub·UBD interactions upon transition to the gas-phase, hence allowing an accurate representation to the degree of binding to be measured. Illustrated in Figure 1a is the ESI mass spectrum of the mono-Ub·UQ1-UBA complex sprayed from 25 mM ammonium acetate. The $[Ub{\cdot}UQ1{-}UBA{+}8H^+]^{8+}$ ion is observed at m/z 1659. Quadrupole isolation of this ion (Supporting Information Figure S2a) shows that it is readily dissociated into its components (Ub 5+ and UQ1-UBA 3+) without elevated collision energy. This is mainly attributed to the relatively high kinetic (and hence internal) energy gained by the 8+ complex ion, and Coulomb repulsion between the charged binding partners. As a consequence the binding strength determined from this spectrum (K_d = 47 μM) was more than 2-fold lower than values reported in the literature (K_d = 20 μM).[17] To prevent facile dissociation of the $[Ub{\cdot}UQ1{-}UBA{+}8H^+]^{8+}$ complex, we sought to lower the

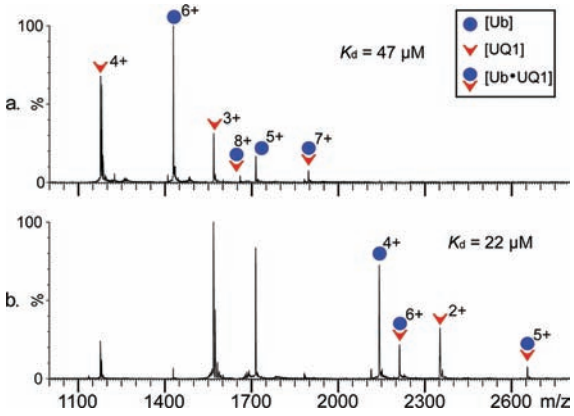

Figure 1. Charge reduction by acetonitrile vapor exposure: (a) ESI mass spectra of UQ1-UBA (4 μM) and mono-Ub (0.5 μM) sprayed from 25 mM ammonium acetate, and (b) ESI mass spectra of UQ1-UBA (4 μM) and mono-Ub (0.5 μM) sprayed from 25 mM ammonium acetate in the presence of acetonitrile vapor, showing the reduction in ionic charge state and the increase in signal of the mono-Ub·UQ1-UBA complex.

charge state of the ions observed. Several approaches have been reported to reduce the charge state of protein ions produced by ESI.[33,41,42] Here we show that exposure of the electrospray plume to acetonitrile vapor,[40] results in the effective reduction of the charge states of Ub, UBDs and their complexes. Illustrated in Figure 1b is the mass spectrum obtained for the mono-Ub·UQ1-UBA complex, electrosprayed from 25 mM ammonium acetate in the presence of acetonitrile vapor. The charge states of the complex were reduced to 6+ and 5+ at m/z 2212 and 2654, respectively. Additionally, no dissociation of the complex was observed post quadrupole isolation of $[Ub{\cdot}UQ1{-}UBA{+}6H^+]^{6+}$ (Supporting Information Figure S2b). The increase in complex stability is principally a result of lowering the kinetic energy transferred to the ions in the mass spectrometer, and a reduction in perturbation of the complex by protonation. Under these conditions, Ub ions ranged from 3+ (m/z 2856) to 6+ (m/z 1428), with 4+ (m/z 2142) and 5+ (m/z 1714) ions found to be the dominant species. K_d values were determined from a titration experiment in which the Ub concentration was fixed at 0.5 μM and the concentration of UQ1-UBA domain was varied from 1 to 8 μM. The mean apparent K_d value determined from these measurements was 22 ± 2 μM, which is in excellent agreement with 20 ± 5 μM from NMR[17] and 27 μM from SPR[18] experiments, and indicates the importance of producing low charge state ions for the survival of weak Ub complexes.

3.2. Quantifying Ub-UBD Binding Affinity. To evaluate the potential of this method further, we tested it against a series of previously studied Ub·UBD complexes, where binding affinities had been determined by other methods, before examining unstudied systems. The UBDs used in this work were classified into two categories: (i) helical UBDs including the single α-helix MIU domain of Rabex-5 (subsequently referred to as MIU) and the three-helix-bundles UQ1-UBA and the C-terminal UBA domain of hHR23A (from here onward refer to as UBA2) and (ii) ZnF domains represented by the IsoT-ZnF. Table 1 shows the K_d values obtained for each Ub·UBD complex. Comparison of values measured by ESI-MS with those taken from the literature (Table 1, values in parentheses) shows an excellent agreement, indicating that the ESI-MS methodology described is suitable for quantifying these

Table 1. Apparent Dissociation Constant (K_d) Values for UBD·(Poly)-Ub Interactions

	K_d (μM)[a]						
UBD	Ub	Lys48-Ub_2	Lys63-Ub_2	Lys11-Ub_2	Lys27-Ub_2	Lys48-Ub_4	Lys63-Ub_4
UQ1-UBA	22 ± 2 (20 ± 5)[17]	15 ± 2 (4 ± 5)[17]	24 ± 2 (18 ± 18)[17]	21 ± 2	35 ± 3	13 ± 2 (1.2)[18]	15 ± 2 (0.5)[18]
UBA2	200 ± 14 (400 ± 100)[20]	18 ± 2 (18 ± 7)[20]	126 ± 18 (210 ± 100)[26]	72 ± 10	81 ± 10	8 ± 1 (7.7)[18]	>70[b] (28)[18]
MIU	36 ± 4 (29 ± 1)[28]	11 ± 2	16 ± 2	12 ± 2	ND	ND	ND
IsoT-ZnF	2.3 ± 0.2 (2.8 ± 0.1)[22]	3.6 ± 0.8	2.8 ± 0.3	1.7 ± 0.2	ND	ND	ND

[a]The K_d values reported here (mean ± SD) were averaged from values measured at different concentrations. Given in parentheses are the previously reported values obtained by NMR or SPR. Where values in parentheses are not given, values have not been previously reported. [b]Complex signal below the limit of detection, which equates to K_d = 70 μM for this system using the available concentration of 0.5 μM. ND, not determined.

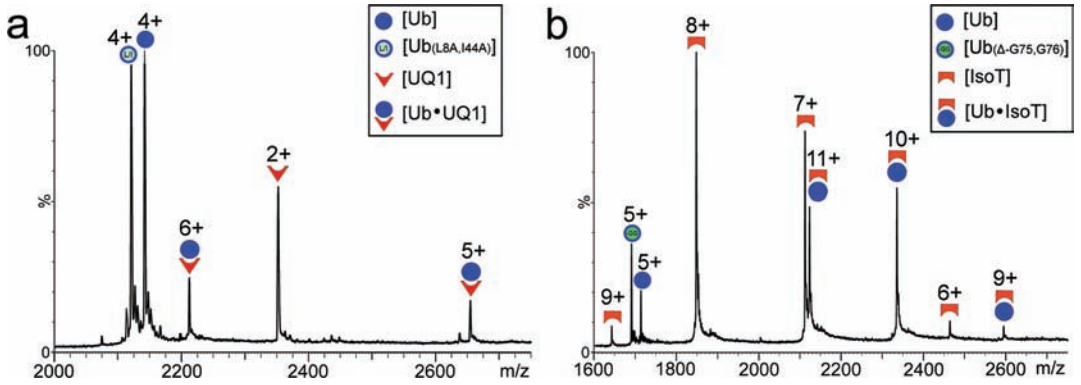

Figure 2. Confirming Ub·UBD interaction specificity. ESI mass spectra of (a) UQ1-UBA (4 μM), wt-Ub (0.5 μM), and Leu8Ala/Ile44Ala-Ub (0.5 μM) in the presence of acetonitrile vapor, and (b) IsoT-ZnF (2 μM), wt-Ub (0.5 μM), and Δ-Gly75/Gly76-Ub (0.5 μM), showing specific binding.

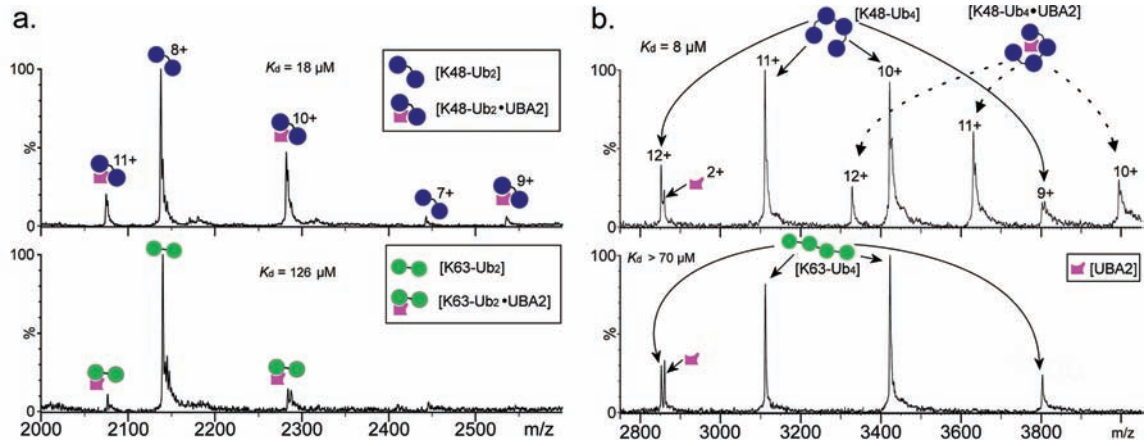

Figure 3. Linkage specificity of the UBA2 domain of hHR23A binding to Lys48 and Lys63-linked poly-Ub chains. ESI mass spectra of UBA2 (4 μM) with (a) di-Ub (0.5 μM) sprayed from 25 mM ammonium acetate and (b) tetra-Ub (0.5 μM).

biologically important interactions. Interestingly, it is not strictly necessary to carry out charge reduction on complexes of IsoT-ZnF (Figure 2b and Supporting Information Figure S3), as both conditions yield almost identical K_d values, which suggests these species are more stable in the gas phase at higher charge state.

The complex between mono-Ub and UBA2 showed the lowest affinity (K_d = 200 ± 14 μM). It should be noted that this value was calculated from the addition of only 4 μM UBA2 to Ub. Such is the nature of MS measurements, however, that even low abundance complex ions are readily detectable in the spectrum and saturation conditions are not required to determine K_d. Indeed the ability to work at low micromolar range better reflects the physiological situation as the cellular concentration of Ub is estimated to be approximately 85 μM.[43] IsoT-ZnF exhibits one of the highest known affinities for Ub (K_d = 2.3 ± 0.2 μM), and based on the sensitivity of our MS instrument we estimate the upper level of affinity quantifiable by this method to be 50−100 nM. The development of more sensitive mass spectrometers will extend this range. Naturally, qualitative analysis is possible at much higher affinities.

3.3. Confirming Ub·UBD Interaction Specificity. The specificity of interactions between Ub and the UBDs was examined and confirmed using two Ub mutants. A Leu8Ala/Ile44Ala double mutant of Ub was used to test the specificity of the single helix and three-helix bundle domains, which are known to bind Ub via its Ile44-centered hydrophobic patch (to which Leu8 is adjacent). Figure 2a shows the mass spectrum obtained for the UQ1-UBA complex with an equimolar mixture of wt-Ub and Leu8Ala/Ile44Ala-Ub, electrosprayed from 25 mM ammonium acetate in the presence of acetonitrile vapor. Formation of the wt-Ub·UQ1-UBA complex was clearly

dx.doi.org/10.1021/ja300749d | J. Am. Chem. Soc. 2012, 134, 6416−6424

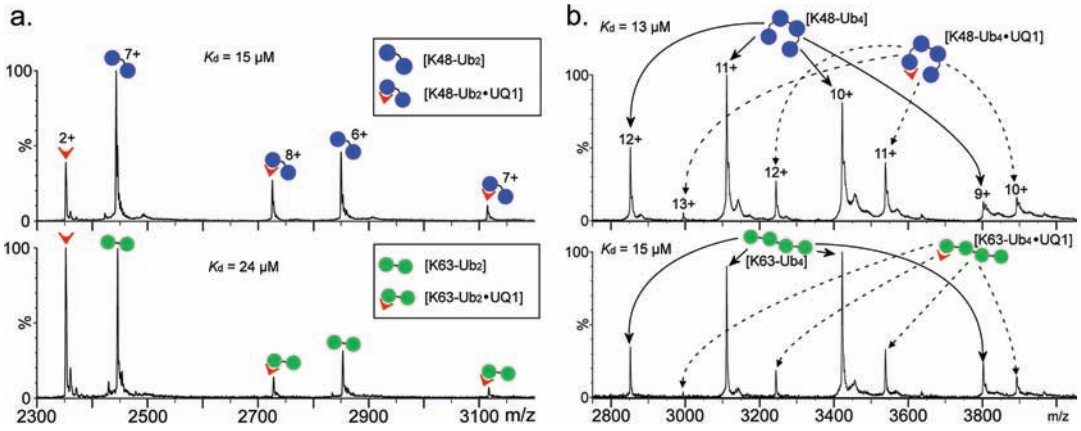

Figure 4. ESI mass spectra of 4 μM UQ1-UBA with (a) 0.5 μM di-Ub and (b) 1 μM tetra-Ub, in the presence of acetonitrile vapor showing the domain's lack of specificity for poly-Ub linkage topology.

detectable as 5+ and 6+ ions (Figure 2a), while the Leu8Ala/Ile44Ala-Ub mutant complex with UQ1-UBA was barely visible. This result demonstrates the requirement for Leu8 and Ile44 in the interaction between Ub and UQ1-UBA, and confirms the specificity of the interaction observed by MS.

Unlike the helical domains, IsoT-ZnF interacts with Ub via the latter's C-terminal residues as reported previously.[22] Comparison of data obtained for IsoT-ZnF domain binding to wt-Ub and a Δ-Gly75/Gly76-Ub mutant in a competition assay showed a clear wt-Ub·IsoT-ZnF complex but no association between Δ-Gly75/Gly76-Ub and the IsoT-ZnF domain (Figure 2b). These results demonstrate the requirement of Gly75 and Gly76 for the interaction of Ub with IsoT-ZnF, and again confirm specificity of Ub·UBD interactions detected by ESI-MS. From these Ub mutant studies it can be concluded that ESI-MS can be used to probe specific mechanisms of Ub recognition.

3.4. Specificity for Poly-Ub Chain Topology. The UBA2 domain of hHR23A is known to demonstrate preferential binding to Lys48-linked poly-Ub over Lys63-linked chains.[14,18−20] Comparison of ESI-MS spectra obtained in this study for UBA2 complexes with mono-Ub (Supporting Information Figure S4) and poly-Ub (Figure 3 and Supporting Information Figure S5), showed that complex formation favored Lys48 linked poly-Ub chains and that this selectivity was most pronounced for this tetra-Ub (Figure 3b). ESI-MS apparent K_d values for UBA2 (Table 1) are in good agreement with previously reported values obtained by NMR.[18,20,26] Additionally, new data for Lys11 and Lys27 di-Ub·UBA2 interactions are provided for the first time. Affinities for these linkage topologies are also significantly weaker than for Lys48 di-Ub. It is notable that charge reduction is again not absolutely required to stabilize complexes between the UBA2 with di-Ub and tetra-Ub chains, as similar apparent K_d values were obtained with and without exposure to acetonitrile vapor. Charge reduction does, however, have the advantage of simplifying the spectrum of UBA2 and tetra-Ub by preventing signal overlap.

In contrast to the linkage specificity evident for the UBA2 domain, it has been reported that the UQ1-UBA domain shows little binding selectivity between Lys48 di-Ub and Lys63 di-Ub chains.[17] ESI-MS of UQ1-UBA complexes with mono-Ub (Figure 1b), Lys48 di-Ub, Lys63 di-Ub, Lys48 tetra-Ub and Lys63 tetra-Ub (Figure 4) showed little or no binding preference for poly-Ub chain topology. Measured apparent K_d values for these complexes (Table 1) were found to be similar in value. Lys11 di-Ub and Lys27 di-Ub binding data are presented for the first time (Supporting Information Figure S6). Here again, little binding preference was exhibited. These data are consistent with one UQ1-UBA molecule binding at only a single Ile44 patch on a di-Ub unit, as suggested by NMR. In agreement with ESI-MS, the previous NMR study concluded that intermolecular contacts between the UQ1-UBA and the individual Ubs in these chains (di-Lys48 and di-Lys63 units) are practically the same as with mono-Ub.[17] The tetra-Ub complexes measured here are somewhat weaker than the values previously determined by SPR.[18] However, given that the SPR experiments were conducted on dimeric GST-UQ1-UBA fusions, artifactual chelate effects leading to apparently higher affinity with longer poly-Ub chains are a likely explanation of this discrepancy. Indeed, this effect has previously been observed with GST-UBD fusion proteins.[44]

In addition to validating ESI-MS methodology against known Ub interactions we have provided new insights into binding affinities of previously unstudied complexes (see Table 1). Specifically the Rabex-5 MIU and IsoT-ZnF have been shown to exhibit no linkage specificity for the di-Ub linkages examined. The preference of UBA2 for Lys48 di-Ub over not only Lys63 di-Ub but also Lys11 di-Ub and Lys27 di-Ub has also been demonstrated for the first time.

The complex formed between the IsoT-ZnF and commercial Lys48 di-Ub revealed an interesting phenomenon. Calculation of the apparent K_d based on the signal intensities of the major species in the ESI spectrum (Supporting Information Figure S7) gave an initial value of 20 μM (almost 6-fold higher than that subsequently described). Further investigation revealed that the commercial Lys48 di-Ub contained a significant quantity of cyclic material. This product forms during *in vitro* synthesis due to the close spatial proximity of the proximal Ub's C-terminus and Lys48 of the distal Ub.[45] The absence of a free C-terminus in cyclic Lys48 di-Ub would prevent it from binding to IsoT-ZnF, which requires a flexible and free Gly75/Gly76 motif. Indeed, examination of the ESI spectrum for this system showed a complex for acyclic Lys48 di-Ub·IsoT-ZnF only (measured mass for Lys48 di-Ub complex = 31 893 Da, theoretical masses for cyclic and acyclic Lys48 di-Ub complexes = 31 876 and 31 894 Da, respectively, see Supporting Information Figure S7). Calculation of apparent K_d based on the acyclic population provided the value of 3.6 ± 0.8 μM,

dx.doi.org/10.1021/ja300749d | J. Am. Chem. Soc. 2012, 134, 6416−6424

which is in line with values for mono-Ub and the other di-Ub linkages (1.7−2.8 μM).

The discovery of cyclic material within the Lys48 di-Ub used caused us to re-examine our findings for UQ1-UBA, UBA2 and MIU interacting with this form of di-Ub. Interestingly, calculations of apparent K_d values based on either cyclic or acyclic populations made little or no difference to the values (Supporting Information Table S2). This demonstrates that these UBDs have no specificity for binding cyclic or acyclic Lys48 di-Ub.

3.5. Multisite Binding of Ub to UBDs. Having established that ESI-MS measurements are able to detect specific interactions between Ub and a range of UBDs we postulated that the method could be expanded to examine multiple domain interactions with different Ub site specificities. We have recently modeled members of all 20 known families of UBDs to assess the likelihood of Ub-mediated ternary complex formation.[46] We tested our predictions using UQ1-UBA and IsoT-ZnF domains which our analyses indicated should be able to form a ternary Ub·UQ1-UBA·IsoT-ZnF complex, where different binding patches on Ub are utilized. ESI-MS of a mixture of the three components did, indeed, lead to a clearly detectable ternary complex (Figure 5), confirming that multiple

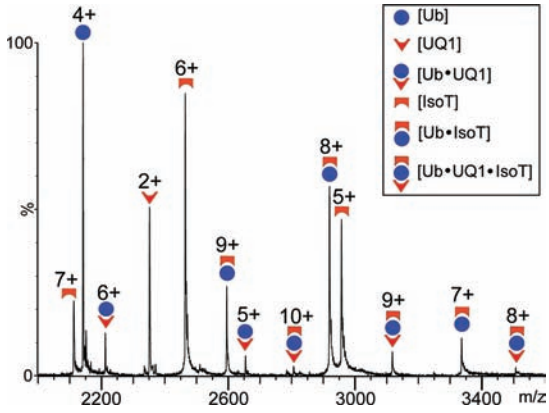

Figure 5. Multisite binding of Ub to UBDs. ESI mass spectrum of 0.5 μM mono-Ub with 4 μM UQ1-UBA and 2 μM IsoT-ZnF, in the presence of acetonitrile vapor, showing the presence of a Ub·UQ1-UBA·IsoT-ZnF ternary complex.

UBDs can bind mono-Ub or poly-Ub simultaneously.[46] The ability of ESI-MS to visualize interactions between mono-Ub (and poly-Ub) with multiple UBDs opens the way for studying crosstalk between different Ub-dependent pathways, which are difficult to probe using other biophysical techniques.

4. DISCUSSION

4.1. Fidelity of the MS Method. The ESI-MS approach described herein provides a new, rapid and highly sensitive tool for studying the affinity and specificity of Ub·UBD complexes. The results presented reveal several significant new findings for these important regulatory interactions. The approach requires only the measurement of the ratio of the total intensity of the bound and unbound Ub ions formed by the electrospray process and the knowledge of the initial concentration of Ub and UBD. Among the key advantages of this method are the speed of analysis (in an optimized instrument the analysis can be completed within minutes), the low sample consumption (less than 50 μL of sample at micromolar concentration is required for a single measurement), sensitivity (weak and low abundance complexes can be detected without the need of saturation, as demonstrated in case of the UBA2 complex with Ub), and selectivity.

The method uses a titration strategy in which the concentration of the Ub component is fixed to 0.5 μM and the concentration of UBD varies from 1 to 8 μM. Although, the concentration of UBD could be increased, we have demonstrated that the sensitivity of the method allows a very weak interaction between mono-Ub and UBA2 (K_d = 200 μM) to be determined by the addition of only 4 μM of the UBD. In addition, in the cases of the UQ1-UBA and UBA2 domains we have also observed that increasing the domain concentration above 6 μM resulted in the formation of a significant amount of UBD homodimer, which may affect precise determination of K_d. Therefore in order to simplify calculations, we have used domain concentrations closer to those experienced physiologically in which no dimer or negligible amounts of dimer will be formed.

The experiments were performed on a SYNAPT HDMS instrument, with ion mobility-mass spectrometry (IM-MS) capability. Although the use of IM-MS is not essential for the determination of K_d values, it demonstrates some clear benefits. For example, in the case of Ub·UBA2, the unbound mono-Ub ion 3+, the unbound domain ion 2+ and the complex ion 5+, show m/z values of 2856, 2858, and 2857, respectively, which are almost impossible to discriminate in the mass spectrometer. The problem is overcome by the use of IM-MS, which has the additional ability to separate ions based on their mobility through a buffer gas, providing a second dimension for resolution of isobaric or near-isobaric species.

To ensure that our data were not affected by artifacts related to the ionization or detection process, we conducted a series of experiments to test the fidelity of our results. First, we took steps to minimize disruption of non-covalent complexes in the mass spectrometer. For several complexes it was essential to reduce the charge state distribution of the ions. Lower charge states were obtained by exposure of the electrospray plume to acetonitrile vapor. Where there are concerns over complex stability we recommend the use of charge reduction by acetonitrile vapor exposure, but it is not essential in every case. Second, the specificity of the observed non-covalent complex was tested and confirmed by a competitive binding assay using wild-type and mutant Ubs. Complexes were selectively formed with wt-Ub for both the three-helix-bundle and ZnF-type UBDs, which confirmed the specificity of the signals detected. It is still unclear whether these native solution intermolecular protein interactions are the most significant forces in maintaining the complex post desolvation. This consideration, while interesting, is essentially irrelevant for the successful application of the method, providing the complex remains associated from the moment of desolvation to the point of detection. Any rearrangement to a more stable gas-phase structure would not affect the fidelity of the measurements. Recently it has been suggested that Ub does maintain its native folded structure in the gas phase,[47] which may mean that Ub·UBD complexes are also solution-like in this environment.

A third potential issue in using ESI-MS to quantify protein−protein interactions is the response factors for the bound and unbound ions. The response factor of a protein is related to its ionization efficiency which, in turn, is linked to its effective hydrophobicity in solution. Formation of protein−protein complexes in solution can be associated with conformational

dx.doi.org/10.1021/ja300749d | J. Am. Chem. Soc. 2012, 134, 6416−6424

changes. If the free state of a protein is partially unfolded compared to the complex form, then its effective hydrophobicity will be enhanced. Such a scenario will increase the ionization efficiency of the free protein and thus the response factors of unbound and bound protein ions will be dissimilar.[38] Since interactions between Ub and UBDs will bury a small number of hydrophobic residues on both proteins, we sought to establish whether this affected the electrospray behavior of the complex relative to its component proteins. Kaltashov and Mohimen have shown that for natively folded proteins there is a linear relationship between ln(average ESI charge state) and ln(surface area, Å^2) with a slope of 0.69 ± 0.02.[48] Using the logic developed by Liu and Konermann[38] significant departure from this relationship may indicate changes in ionization efficiency brought about by exposure or burial of hydrophobic residues caused resulting from protein−protein association. Plotting ln(average ESI charge state) versus ln(surface area, Å^2) for mono-Ub and the four complexes investigated in this paper, resulted a straight line with a slope of 0.68 ± 0.01 (Supporting Information Figure S8), which is in excellent agreement with the value reported by Kaltashov and Mohimen.[48] Thus, we conclude that formation of Ub·UBD complexes is not linked with major conformational changes in the subunits, consistent with previously reported data from solution studies,[17] and that burial of a relatively small number of hydrophobic residues does not appear to impact upon ionization properties of the complex compared to the unbound Ub.

Perhaps the most compelling evidence for the applicability of the ESI-MS approach for studying Ub·UBD complexes is the excellent agreement achieved between these affinity data and those of other biophysical methods. When tested against a series of previously studied Ub·UBD complexes the MS results were found to be in an excellent agreement with the K_d values that have been previously determined.

4.2. New Insights. New insights into Ub·UBD interactions by the application of this methodology have been described, including the discovery that UBA2 from hHR23A has a preference for Lys48 di-Ub over the Lys11 and Lys27 linkages, as well as over the Lys63 form. We have also shown that the UQ1-UBA, Rabex-5 MIU and IsoT-ZnF domains have little or no specificity for the linkages examined—binding each with similar affinity. The discovery that Ub is able to bind both UQ1-UBA and IsoT-ZnF domains simultaneously is a direct test of the prediction made by Garner et al.[46] Our finding that IsoT-ZnF is unable to bind cyclic Lys48 di-Ub is consistent with the importance of a free C-terminus for poly-Ub association with this domain, and subsequent deubiquitination by the IsoT enzyme. The ability of the remaining domains tested to interact with cyclic and acyclic Lys48 di-Ub with similar affinities suggests that cyclic Lys48 di-Ub may have hitherto uncharacterized role in Ub-signaling. Interestingly, we have recently identified the presence of endogenous cyclic Lys48 di-Ub in rat skeletal muscle and mammalian cultured cells (to be reported elsewhere), which demonstrates that this form of di-Ub is generated *in vivo*.

4.3. Comparison with Other Biophysical Methods. As outlined in the introduction, previous work has used NMR, SPR, ITC and FA to examine Ub·UBD interactions. A comparison of their requirements and limitations is set out, alongside those of MS, in Supporting Information Table S3. Like most of the techniques available MS covers the affinity range seen for most Ub·UBD complexes. But, unlike NMR and ITC, MS can measure these interactions at physiological concentrations (low micromolar). SPR exhibits similar sensitivity to MS, but with the drawback of requiring immobilization of one binding partner. This can lead to underestimation of affinity through loss of activity, or overestimation of affinity through artifactual avidity effects.[44] FA is also generally considered a sensitive method for probing protein−protein interactions, but this sensitivity is lost for affinities in the >10 μM range. This is a serious drawback for Ub·UBD complexes. Moreover, FA requires the labeling of one binding partner, which may interfere with association. In cases where no structural data is available, and the binding sites are not characterized, this is a serious consideration. Additionally, FA requires a significant difference in relative molecular mass of the labeled protein and its unlabeled partner. This is often not the case in Ub·UBD complexes (e.g., di-Ub·IsoT-ZnF). For these reasons, FA has been relatively rarely used in the UBD field, and only when binding-site information was available and when a considerable difference in the sizes of the Ub and UBD partners was present.[29,44] Like SPR and ITC, FA relies on relatively complex data analysis, often with uncertainties over stoichiometry. In contrast, MS gives clear stoichiometry information.

The power of MS, underlying its advantages over techniques such as SPR, ITC and FA, lies in the fact that it (i) gives discrete signals for *all* species present and (ii) provides structural information on each species by mass measurement. Through this ability, MS is able to identify the presence of interactions between *all* binding partners, as well as their stoichiometry. For example, the UBA domain of p62 exists in a concentration-dependent monomer−dimer equilibrium.[49] Addition of Ub, results in the formation of a competing Ub·p62-UBA heterodimer. All the components of this dynamic ensemble are readily detected by MS, without prior knowledge, but would remain unseen by SPR, ITC and FA. Indeed, depending on the protein concentrations used, ITC and FA may give misleading results. In this paper we report the detection of an unexpected cyclic Lys48 di-Ub impurity in commercial Lys48 di-Ub, and demonstrate its inability to bind to IsoT-ZnF. This phenomenon was clearly apparent by MS, but would have remained undetected by the other biophysical methods. Instead an inaccurate affinity would have been recorded, with the error dependent upon the relative ratio of cyclic and acyclic Lys48 di-Ub components. The capability of MS readily to detect and identify unknown and unexpected components in a mixture of binding partners adds a degree of confidence to the measurements which is unmatched by all but NMR structural assignment. Uniquely, ternary and higher-order complexes, as well as their sub-complexes are easily detected by MS.

The analysis time for MS measurement compares favorably with other biophysical methods. The mass spectrometer requires optimization and tuning for detection of Ub·UBD complexes only once. This takes approximately 1 day. The instrument parameters can be saved and recalled when required. Identical parameters were used for the detection of all complexes studied in this study. The only variable was the need for charge reduction of some complexes, but since this has no affect on the measured affinities, solvent exposure could be used as a matter of course. Single measurements of a complex typically take less than 10 min each, and are straightforward to perform with a little experience in instrument operation. Use of automated MS source interfaces, such as the Advion NanoMate, permits high-throughput screening of Ub·UBD com-

plexes, and their inhibition, with each automated measurement requiring approximately 2 min. A 384-well plate can be screened in 13 h using this approach.

The capital cost of a mass spectrometer is relatively high, but many chemistry and biochemistry departments are equipped with ESI-MS instrumentation capable of conducting these studies. Indeed, it is now becoming common practice to characterize recombinant proteins by routine MS mass measurement using just such an instrument. This is particularly advisible when checking for the incorporation of a fluorescent tag, for example. As the MS method itself consumes very small quantities of untagged proteins, the per sample cost is very low. For these reasons we do not believe that MS compares unfavorably with other biophysical methods on cost. Given the advantages it affords in sensitivity, speed and quality of information, MS shows great promise in probing biologically relevant multivalent interactions with (poly)Ub. The need for new, highly sensitive methods to understand the specificity and dynamics of the ubiquitin system has recently been highlighted by Ikeda et al.[50] As just one example it could provide further insights in to how the UBDs of proteasome subunits Rpn13 and Rpn10 cooperate to function as a "molecular ruler" effectively sensing the length of poly-Ub chains delivered to the proteasome.[51,52]

■ ASSOCIATED CONTENT

Supporting Information

Further mass spectra, individual cyclic and acyclic Lys48 di-Ub K_d values, and charge state vs surface area plot for the UBD complexes studied. This material is available free of charge via the Internet at http://pubs.acs.org.

■ AUTHOR INFORMATION

Corresponding Author

neil.oldham@nottingham.ac.uk

Notes

The authors declare no competing financial interest.

■ ACKNOWLEDGMENTS

This work was funded by the Biotechnology and Biological Sciences Research Council (BBSRC; Grants BB/F019297/1 and BB/F013663/1). The authors are grateful to Kevin Butler for technical assistance.

■ REFERENCES

(1) Elsasser, S.; Finley, D. *Nat. Cell Biol.* **2005**, *7*, 742−749.
(2) Raiborg, C.; Bache, K. G.; Gillooly, D. J.; Madshus, I. H.; Stang, E.; Stenmark, H. *Nat. Cell Biol.* **2002**, *4*, 394−398.
(3) Staub, O.; Rotin, D. *Physiol. Rev.* **2006**, 669−707.
(4) Huang, T. T.; D'Andrea, A. D. *Nat. Rev. Mol. Cell Biol.* **2006**, *7*, 323−334.
(5) Haglund, K.; Dikic, I. *Embo J.* **2005**, *24*, 3353−3359.
(6) Hershko, A.; Ciechanover, A.; Varshavsky, A. *Nat. Med.* **2000**, *6*, 1073−1081.
(7) Pickart, C. M. *Annu. Rev. Biochem.* **2001**, *70*, 503−533.
(8) Chau, V.; Tobias, J. W.; Bachmair, A.; Marriotr, D.; Ecker, D. J.; Gonda, D. K.; Varshavsky, A. *Science* **1989**, *243*, 1576−1583.
(9) Cook, W. J.; Jeffrey, L. C.; Carson, M.; Chen, Z.; Pickart, C. M. *J. Biol. Chem.* **1992**, *267*, 16467−16471.
(10) Sun, L.; Chen, Z. J. *Curr. Opin. Cell Biol.* **2004**, *16*, 119−126.
(11) Hicke, L.; Dunn, R. *Annu. Rev. Cell Dev. Biol.* **2003**, *19*, 141−172.
(12) Spence, J.; Gali, R. R.; Dittmar, G.; Sherman, F.; Karin, M.; Finley, D. *Cell* **2000**, *102*, 67−76.
(13) Massey, L. K.; Mah, A. L.; Ford, D. L.; Miller, J.; Liang, J.; Doong, H.; Monteiro, M. J. *J. Alzheimers Dis.* **2004**, *6*, 79−92.
(14) Raasi, S.; Pickart, C. M. *J. Biol. Chem.* **2003**, *278*, 8951−8959.
(15) Brignone, C.; Bradley, K. E.; Kisselev, A. F.; Grossman, S. R. *Oncogene* **2004**, *23*, 4121−4129.
(16) Walters, K. J.; Lech, P. J.; Goh, A. M.; Wang, Q.; Howley, P. M. *Proc. Natl. Acad. Sci. U.S.A.* **2003**, *100*, 12694−12699.
(17) Zhang, D.; Raasi, S.; Fushman, D. *J. Mol. Biol.* **2008**, *377*, 162−180.
(18) Raasi, S.; Varadan, R.; Fushman, D.; Pickart, C. M. *Nat. Struct. Mol. Biol.* **2005**, *12*, 708−714.
(19) Raasi, S.; Orlov, I.; Fleming, K. G.; Pickart, C. M. *J. Mol. Biol.* **2004**, *341*, 1367−1379.
(20) Varadan, R.; Assfalg, M.; Raasi, S.; Pickart, C.; Fushman, D. *Mol. Cell* **2005**, *18*, 687−698.
(21) Penengo, L.; Mapelli, M.; Murachelli, A. G.; Confalonieri, S.; Magri, L.; Musacchio, A.; Di Fiore, P. P.; Polo, S.; Schneider, T. R. *Cell* **2006**, *124*, 1183−1195.
(22) Reyes-Turcu, F. E.; Horton, J. R.; Mullally, J. E.; Heroux, A.; Cheng, X.; Wilkinson, K. D. *Cell* **2006**, *124*, 1197−1208.
(23) Hoeller, D.; Dikic, I. *Nature* **2009**, *458*, 438−444.
(24) Garner, T. P.; Long, J.; Layfield, R.; Searle, M. S. *Biochemistry* **2011**, 4665−4674.
(25) Trempe, J.-F. *Curr. Opin. Struct. Biol.* **2011**, *21*, 792−801.
(26) Varadan, R.; Assfalg, M.; Haririnia, A.; Raasi, S.; Pickart, C.; Fushman, D. *J. Biol. Chem.* **2004**, *279*, 7055−7063.
(27) Long, J.; Garner, T. P.; Pandya, M. J.; Craven, C. J.; Chen, P.; Shaw, B.; Williamson, M. P.; Layfield, R.; Searle, M. S. *J. Mol. Biol.* **2010**, *396*, 178−194.
(28) Lee, S.; Tsai, Y. C.; Mattera, R.; Smith, W. J.; Kostelansky, M. S.; Weissman, A. M.; Bonifacino, J. S.; Hurley, J. H. *Nat. Struct. Mol. Biol.* **2006**, *13*, 264−271.
(29) Kulathu, Y.; Akutsu, M.; Bremm, A.; Hofmann, K.; Komander, D. *Nat. Struct. Mol. Biol.* **2009**, *16*, 1328−1330.
(30) Daniel, J. M.; Friess, S. D.; Rajagopalan, S.; Wendt, S.; Zenobi, R. *Int. J. Mass Spectrom.* **2002**, *216*, 1−27.
(31) Heck, A. J. R.; Van Den Heuvel, R. H. H. *Mass Spectrom. Rev.* **2004**, *23*, 368−389.
(32) Liu, L.; Bagal, D.; Kitova, E. N.; Schnier, P. D.; Klassen, J. S. *J. Am. Chem. Soc.* **2009**, *131*, 15980−15981.
(33) Bagal, D.; Kitova, E. N.; Liu, L.; El-Hawiet, A.; Schnier, P. D.; Klassen, J. S. *Anal. Chem.* **2009**, *81*, 7801−7806.
(34) Loo, J. A.; Berhane, B.; Kaddis, C. S.; Wooding, K. M.; Xie, Y.; Kaufman, S. L.; Chernushevich, I. V. *J. Am. Soc. Mass Spectrom.* **2005**, 998−1008.
(35) Loo, J. A.; Hu, P.; McConnell, P.; Mueller, W. T.; Sawyer, T. K.; Thanabal, V. *J. Am. Soc. Mass Spectrom.* **1997**, *8*, 234−243.
(36) Clark, S. M.; Konermann, L. *Anal. Chem.* **2004**, *76*, 7077−7083.
(37) Robinson, C. V.; Chung, E. W.; Kragelund, B. B.; Knudsen, J.; Aplin, R. T.; Poulsen, F. M.; Dobson, C. M. *J. Am. Chem. Soc.* **1996**, *118*, 8646−8653.
(38) Liu, J.; Konermann, L. *J. Am. Soc. Mass Spectrom.* **2011**, *22*, 408−417.
(39) Long, J.; Gallagher, T. R. A.; Cavey, J. R.; Sheppard, P. W.; Ralston, S. H.; Layfield, R.; Searle, M. S. *J. Biol. Chem.* **2008**, *283*, 5427−5440.
(40) Hopper, J. T. S.; Sokratous, K.; Oldham, N. J. *Anal. Biochem.* **2012**, *421*, 788−790.
(41) Winger, B. E.; Light-Wahl, K. J.; Smith, R. D. *J. Am. Soc. Mass Spectrom.* **1992**, *3*, 624−630.
(42) Pagel, K.; Hyung, S.-J.; Ruotolo, B. T.; Robinson, C. V. *Anal. Chem.* **2010**, *82*, 5363−5372.
(43) Kaiser, S. E.; Riley, B. E.; Shaler, T. A.; Trevino, R. S.; Becker, C. H.; Schulman, H.; Kopito, R. R. *Nat. Methods* **2011**, *8*, 691−696.
(44) Sims, J. J.; Haririnia, A.; Dickinson, B. C.; Fushman, D.; Cohen, R. E. *Nat. Struct. Mol. Biol.* **2009**, *16*, 883−889.
(45) Hirano, T.; Serve, O.; Yagi-utsumi, M.; Takemoto, E.; Hiromoto, T.; Satoh, T.; Mizushima, T.; Kato, K. *J. Am. Soc. Mass Spectrom.* **2011**, *286*, 37496−37502.

(46) Garner, T. P.; Strachan, J.; Shedden, E. C.; Long, J. E.; Cavey, J. R.; Shaw, B.; Layfield, R.; Searle, M. S. *Biochemistry* **2011**, *50*, 9076−9087.
(47) Wyttenbach, T.; Bowers, M. T. *J. Phys. Chem. B* **2011**, *115*, 12266−12275.
(48) Kaltashov, I. A.; Mohimen, A. *Anal. Chem.* **2005**, *77*, 5370−5379.
(49) Long, J.; Garner, T. P.; Pandya, M. J.; Craven, C. J.; Chen, P.; Shaw, B.; Williamson, M. P.; Layfield, R.; Searle, M. S. *J. Mol. Biol.* **2010**, *396*, 178−194.
(50) Ikeda, F.; Crosetto, N.; Dikic, I. *Cell* **2010**, *143*, 677−681.
(51) Zhang, N.; Wang, Q.; Ehlinger, A.; Randles, L.; Lary, J. W.; Kang, Y.; Haririnia, A.; Storaska, A. J.; Cole, J. L.; Fushman, D.; Walters, K. J. *Mol. Cell* **2009**, *35*, 280−290.
(52) Chen, X.; Lee, B.-H.; Finley, D.; Walters, K. J. *Mol. Cell* **2010**, *38*, 404−415.